Distributed Space-Time Codes for Full-Duplex IR-UWB Amplify-and-Forward Cooperation

Chadi Abou-Rjeily, *Senior Member IEEE*

***Abstract*—In this paper, we consider the problem of full-duplex (FD) relaying in the context of impulse-radio ultra-wideband (IR-UWB) communications. In particular, we propose two novel distributed space-time block codes (STBCs) suitable for the amplify-and-forward (AF) cooperation protocol with one and two relays. Despite the fact that FD relaying results in significant levels of interference between the transmit and receive antennas of each relay, it introduces new concepts to the problem of distributed STBC design. Compared to half-duplex (HD) STBC, FD-STBC is subject to an additional constraint that imposes the structure of the codewords while it offers the predominant advantage that resides in the possibility of including a smaller number of information symbols per codeword for achieving a full rate. We take advantage of this potential for constructing fully-diverse, full-rate and totally-real IR-UWB FD-STBCs that outperform the existing HD-STBCs for all practical levels of the residual self loop interference. In fact, for the sake of transmitting at full rate, the best known distributed HD-STBCs for the non-orthogonal AF protocol require the joint encoding/decoding of $4N_r$ symbols where N_r is the number of relays. On the other hand, the proposed FD-STBCs require embedding only $N_r + 2$ symbols per codeword for transmitting at full rate. Following from this fact, not only the decoding complexity is reduced, but also the coding gains are improved resulting in enhanced performance levels.**

***Index Terms*—Ultra-wideband, UWB, PPM, amplify-and-forward, AF, cooperation, full-duplex, space-time.**

I. Introduction

User cooperation is a well-known powerful fading mitigation technique in which the spatial diversity is exploited in a distributed manner by taking advantage of the potential presence of some nodes in the vicinity of the communicating terminals. Early research in this area targeted the half-duplex (HD) operation mode where the communicating relays need to respect the primary constraint of not transmitting and receiving simultaneously in the same frequency band [1]–[4]. In this context, the HD cooperative solutions can be classified into two broad categories; namely, amplify-and-forward (AF) and Decode-and-forward (DF) protocols. While in the first protocol the signal is simply amplified and retransmitted by the relays, the DF schemes involve the decoding of the incoming data streams. More recently, there has been a growing interest in cooperation in the full-duplex (FD) mode where the HD constraint was leveraged and where the FD relays can now transmit and receive at the same time in the same frequency band thus adding new dimensions and capabilities to the cooperative networks [5]–[13]. On the other hand, FD operation is associated with self loop interference (LI) between the transmit and receive antennas of the relays which might jeopardize the advantages of FD relaying in favor of HD relaying. The superiority of FD relaying was reported in numerous contributions in the absence of LI or in the case of perfect LI mitigation [5]–[7]. In the presence of LI, the optimal duplex mode depends on the level of LI, the signal-to-noise ratios (SNRs) at the relay and destination nodes as well as the strength of the direct link [8], [9].

Of particular relevance to this work are the distributed space-time coding (STC) strategies whether in the HD mode such as [3], [4] or in the FD mode such as [11]–[13]. These correspond to non-orthogonal techniques capable of achieving higher spectral efficiencies compared to the orthogonal techniques. In [3], a non-orthogonal amplify-and-forward (NAF) strategy was proposed and proven to achieve the optimal diversity-multiplexing tradeoff (DMT) of the HD cooperative channel. Minimal-delay explicit STBCs based on the HD-NAF protocol were introduced in [4] in the context of narrow-band communications. In [11], several diversity protocols were proposed for the equivalent multiple-input-multiple-output (MIMO) channel obtained in the FD mode for one-relay AF systems. The codewords span several independent realizations of the block fading channel and achieve full diversity in the cases of perfect and imperfect LI cancelation. In [12], an Alamouti-based distributed FD-STBC was considered for DF relaying with one relay where space-time codewords extending over three symbol durations were implemented. Finally, in [13], convolutional STCs were proposed for FD-AF relaying with one relay in the cases of perfect and imperfect LI cancelation. Unlike [11], the time span of the encoding schemes in [12], [13] is confined to the same fading block.

The huge literature on HD-cooperation and FD-cooperation in the context of narrow-band communications [1]–[13] has motivated much research in the direction of investigating these techniques and tailoring them to the context of impulse-radio ultra-wideband (IR-UWB) communications [14]–[21]. In fact, user cooperation leverages the performance and extends the coverage of UWB networks by counterbalancing the detrimental impairments imposed by the nature of propagation of UWB signals and by the stringent regulations imposed on the transmission levels. These contributions highlighted the utility of spatial diversity with UWB systems. In fact, despite the high frequency selectivity of the UWB channels, profiting from the multi-path diversity can necessitate Rake receivers with very high orders. This follows from the very important delay spread of these channels. Moreover, UWB channels are subject to cluster fading where it is not improbable that a large number

The author is with the Department of Electrical and Computer Engineering of the Lebanese American University (LAU), Byblos, Lebanon. (e-mail: chadi.abourjeily@lau.edu.lb).

of consecutive multi-path components have small amplitudes. In this context, the additional spatial degree of freedom can result in higher performance levels, multiplexing gains and communication ranges. However, despite this rich literature on IR-UWB cooperative systems, all considered solutions were in the HD mode and, to the author's best knowledge, the problem of FD relaying was never considered before in the context of UWB communications. In this context, [14]–[21] assumed operation in the HD mode. [14] investigated the bit error rate (BER) performance of single-relay DF cooperation in the context of coherent and differential-transmitted-reference UWB communications in the case where the relay is equipped with multiple antennas. A similar BER analysis of single-relay DF systems was performed in [15] over the IEEE 802.15.4a channel model based on computing the characteristic function of the decision variable at the destination. The expected capacity and outage capacity of the single-relay DF scheme were also derived in [16]. The issues of power allocation and path selection were tackled in [17] in the context of DF noncoherent UWB systems. In [18], an AF cooperation strategy that is based on the orthogonal STBCs was proposed and analyzed in terms of outage probability in the context of dual-hop multi-antenna IR-UWB transmissions. IR-UWB AF cooperation was also studied in [19] where a multiple differential encoding scheme was proposed and analyzed. Of direct relation to this work are the distributed HD-STBCs proposed in [20], [21] that are based on the extension of the algebraic codes in [4] to the context of IR-UWB communications where an additional constraint of having totally-real codewords is imposed.

IR-UWB systems are characterized by the following main features that distinguish them from narrow-band systems from the cooperative communications point of view. (i): The UWB channel is highly frequency selective resulting in a drastically different system model and imposing additional constraints on the processing techniques to be implemented at the relays as will be highlighted later. (ii): IR-UWB transmissions impose a totally-real constraint on the transmitted symbols since it is extremely difficult to control the phases of the sub-nanosecond UWB pulses whose bandwidth extends over several GHz [20]. (iii): IR-UWB systems are often associated with non-conventional modulation schemes such as pulse position modulation (PPM) that differs substantially from QAM and PSK. In this paper, we propose two novel families of distributed FD-STBCs that are suitable for one-relay and two-relay IR-UWB communications with PPM. The proposed FD-STBCs satisfy the desirable constraints of being full-rate, fully-diverse, totally-real and adapted to PPM where the proposed codewords are based on convenient permutation and pulse-combining matrices that achieve diversity taking advantage of the structure of the M-dimensional sparse M-PPM constellations. For the AF-FD protocol under consideration, we prove that it is sufficient to jointly encode N_r+2 symbols where N_r stands for the number of relays. Owing to this small number of symbols to be included in each codeword, the proposed FD-STBCs profit from enhanced coding gains and a reduced decoding complexity where only N_r+2 symbols need to be jointly decoded.

Benchmarking the proposed scheme with the existing IR-UWB cooperative solutions shows the following difference with [14]–[21] in addition to the major difference of operating in the FD mode rather than the HD mode. Unlike [14]–[17] that are based on the DF protocol, the proposed scheme is based on the AF protocol. Unlike [18], [19], the proposed scheme assumes the presence of a direct link between the source and destination which necessitates putting in place a distributed STBC for the sake of appropriately encoding the data streams that are transmitted simultaneously from the source and relay(s) to the destination. Compared to the optimal IR-UWB HD-STBCs based on the NAF protocol [20], [21], the proposed FD-STBCs share the desirable properties of being full-rate, fully-diverse, totally-real and adapted to PPM. On the other hand, even though the NAF protocol is optimal in the sense of achieving the optimal DMT of the channel [3], and even though the corresponding constructed HD algebraic STBCs are minimal-delay [4], [20], [21], the NAF HD-STBCs suffer from the fact that $4N_r$ symbols need to be included in each codeword. This excessive number of symbols results in reduced coding gains especially for large values of N_r. In fact, it is well-known that the coding gain of the algebraic constructions in [4], [20], [21] depends on the number of jointly-encoded symbols (number of dimensions) via the discriminant of the algebraic field extensions (or product distance of the complex constellation rotations), a quantity that decreases rapidly with the number of dimensions. On the other hand, the proposed FD-STBCs encompass only N_r+2 symbols resulting in higher coding gains and reduced decoding complexities compared to the HD-STBCs in [20], [21]. On the other hand, operating in the FD mode imposes a fixed structure on the codewords. This structure differs substantially from the case of the algebraic constructions based on cyclic division algebras rendering these powerful techniques not suitable for the STBC construction problem under consideration.

In the absence of any work on FD IR-UWB cooperation, we will next benchmark our work with the narrow-band FD cooperative systems deploying distributed STBCs [11]–[13] that, in all circumstances, can not be applied with PPM. First, [11]–[13] are limited to one-relay systems while the proposed FD-STBCs can be applied with two relays as well. Compared to [11], our work does not neglect the strength of the source-destination link and the codewords are limited to the same fading block resulting in simple encoding and decoding. Compared to [12], the proposed schemes are full rate. In fact, the proposed FD-STBCs transmit at the rate of one symbol per channel use (i.e. no data rate reduction compared to non-cooperative systems) while the STBC in [12] transmits at the rate of $2/3$ symbols per channel use. Other major differences are that the proposed schemes are based on the AF strategy (not the DF strategy) and can be implemented in the absence of a feedback link to the source node. Finally, compared to [13], the proposed solution corresponds to a block code not a convolutional code.

II. System Model and Cooperation Strategies

A. General Parameters

An appealing modulation scheme for IR-UWB is M-ary PPM where an UWB pulse is transmitted in one out of

M positions. The information symbols are carved from the following M-dimensional signal set:

$$\mathcal{C} = \{e_m \ ; \ m = 1, \ldots, M\} \quad (1)$$

where e_m stands for the m-th column of the $M \times M$ identity matrix I_M.

We denote by N_r the number of relays and we consider IR-UWB communications with $N_r = 1$ and $N_r = 2$ full-duplex relays as depicted in Fig. 1 and Fig. 2. The relays will be denoted by R_1-R_{N_r} whereas the source (S) and destination (D) nodes will be denoted by R_0 and R_{N_r+1}, respectively. S and D are equipped with one antenna each while the relays are equipped with two antennas (one for reception and the other for transmission) to implement a FD operation mode. L-finger Rake receivers are deployed at the relays and the destination in order to capture the multi-path diversity and we consider the general case where a direct link is present between S and D.

The channel between the n-th and n'-th nodes is described by the $LM \times M$ matrix $H_{n,n'}$ whose elements can be written as [20]:

$$H_{n,n'}((l-1)M+m, m') = \sqrt{\rho_{n,n'}} h_{n,n'}\left((m-m')\delta + \Delta_l\right) \ ; \ l = 1, \ldots, L \ ; \ m, m' = 1, \ldots, M \quad (2)$$

which reflects the impact of the signal transmitted by node R_n during the m'-th position on the m-th correlator (corresponding to the m-th position) placed after the l-th Rake finger of node $\mathrm{R}_{n'}$. In (2), δ stands for the modulation delay and Δ_l for the l-th finger delay. Moreover, $h_{n,n'}(\tau) = \int_0^{T_w} g_{n,n'}(t) w(t-\tau) \mathrm{d}t$ where $w(t)$ is the UWB pulse waveform of duration T_w while $g_{n,n'}(t)$ stands for the convolution of $w(t)$ with the impulse response of the frequency selective channel between nodes n and n'. For $n \neq n'$, $\rho_{n,n'}$ in (2) is the path-loss of the link R_n-$\mathrm{R}_{n'}$ normalized by that of the direct link S-D. In other words, this coefficient is introduced to reflect the fact that the distances between the communicating nodes are not necessity the same as the distance between S and D. In particular, this coefficient takes the value: $\rho_{n,n'} = \left(\frac{d_{0,N_r+1}}{d_{n,n'}}\right)^{n_{\text{path}}}$ where $d_{i,j}$ stands for the distance between nodes R_i and R_j (d_{0,N_r+1} is the distance between S and D and $\rho_{0,N_r+1} = 1$) while n_{path} is the pathloss exponent along the UWB channel (that assumes values between 1.5 and 5 [22]). Note that for two-relay systems, $\rho_{1,2} = \rho_{2,1}$ since the transmit and receive antennas of each relay are separated by a short distance. No reference to the Time-Hopping (TH) sequence was made since multiuser interference is not considered in this work. In this context, it is assumed that the source and relays share the same pseudo-random TH sequence (initially reserved to the source) thus resulting in the same average interference as in the case of non-cooperative IR-UWB TH networks. The proposed solution can also be applied with high data-rate IR-UWB systems that can be deployed in the absence of TH pulse repetitions.

Setting the narrowband FD systems as a reference, common models for the residual self loop interference consist of either attributing a SNR-independent value not greater than one to $\rho_{n,n}$ as in [13], [23] or the SNR-dependent value $SNR^{-\mu}$ where $\mu \geq 0$ as in [11], [12]. In the absence of any research on the self loop interference mitigation in the UWB context, we set $\rho_{n,n} = 1$ which corresponds to the extreme case scenario that holds whether with the first model ($\rho_{n,n}$ is constant) or with the second model with $\mu = 0$. In this case, we are assuming that a practical non-ideal self interference mitigation procedure (that reduces this kind of interference but does not completely eliminate it) is implemented at the relays. The design of such procedure in the considered UWB context falls beyond the scope of this work.

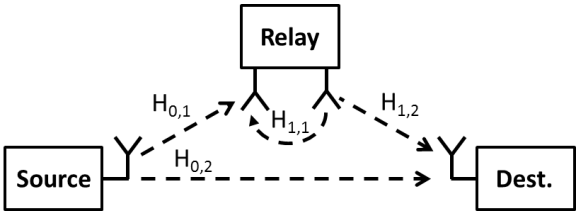

Fig. 1. Full-Duplex cooperation with one relay.

For the inter-relay link when $N_r = 2$, $H_{1,2}$ (resp. $H_{2,1}$) stands for the channel matrix from the transmit antenna of R_1 (resp. R_2) to the receive antenna of R_2 (resp. R_1) where $H_{1,2} \neq H_{2,1}$ since $g_{1,2}(t) \neq g_{2,1}(t)$ as shown in Fig. 2. On the other hand, $H_{n,n}$ represents the loop interference channel from the n-th relay output to its input for $n = 1, 2$ following from the FD operation mode. Given the strong line-of-sight (LOS) between the transmit and receive antennas of a certain relay, the impulse responses $g_{1,1}(t)$ and $g_{2,2}(t)$ are generated according to the IEEE 802.15.3a channel model recommendation CM1 that corresponds to LOS conditions [22]. On the other hand, for $n \neq n'$, the impulse responses $g_{n,n'}(t)$ are generated based on CM2 that corresponds to non-line-of-sight (NLOS) conditions. Note that the structure of HD networks is similar to that provided in figures 1 and 2 where the two antennas at each relay need to be merged into one antenna; that is we set $H_{1,1} = H_{2,2} = 0$. In Fig. 2, $H_{1,2} = H_{2,1}$ given that each relay is now equipped with a single antenna.

For the implementation of a distributed STBC scheme, the transmissions from the source and relays are organized into blocks where each block spans a certain number of symbol durations also referred to as slots. The role of the relay during a certain slot consists of transmitting a processed version of the signal it received in previous slot(s). For AF cooperation over narrow-band channels, the processing is limited to amplifying the incoming signal prior to retransmission. On the other hand, for the highly frequency selective UWB channels, the processing at the relay must also comprise a combining scheme such as maximum-ratio-combining (MRC) [18]–[21]. MRC is carried out in order to avoid excessive additional delay spreads at the destination. In the absence of a combining scheme, the signal energy would be further spread over an increased number of multi-path components resulting in less efficient energy raking and in enlarged symbol durations to eliminate inter-symbol-interference (ISI) [18]–[21]. In a way similar to these references that perform combining at the relays but are nevertheless labeled as AF protocols, the scheme proposed in this paper will also be classified as an AF scheme in order

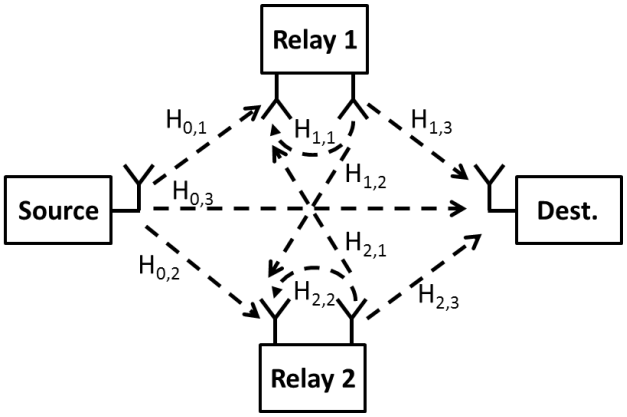

Fig. 2. Full-Duplex cooperation with two relays.

to clearly benchmark this work with the existing contributions in the literature. Note that irrespective of whether MRC is performed or not, the structure of the proposed codewords will remain unchanged since, in all circumstances, these codewords are designed to respect the rank criterion.

The signal received at the n-th relay during the k-th symbol duration is represented by the LM-dimensional vector $Y_k^{(n)}$. In the same way, Z_k represents the LM-dimensional decision vector at D during the k-th symbol duration. For a relay processing that involves amplification and MRC, the signal transmitted by the n-th relay during the k-th slot can be written as:

$$X_k^{(n)} = \Psi_n H_{0,n}^T Y_{k'}^{(n)} \ ; \ k > k' \tag{3}$$

where $X_k^{(n)}$ is a M-dimensional vector, Ψ_n stands for the $M \times M$ amplifying matrix at the n-th relay and the multiplication by $H_{0,n}^T$ ensures coherent combining of the useful signal energy along the link S-R$_n$. Note that over a ceratin slot R$_n$ can remain idle and $X_k^{(n)} = 0_M$ in this case where 0_M stands for the M-dimensional all-zero vector.

A processing delay that does not exceed one symbol duration is strongly justified given the order of magnitudes of the different parameters under consideration. In fact, from (2), the energy raking process extends over the interval $[0 \quad \Delta_L + (M-1)\delta]$ (where the origin of time is taken at the beginning of the symbol duration). Given that the values of Δ_L and δ are comparable to the pulse width T_w that is in the order of 1 ns while the symbol duration T_s is in the order of 100 ns in order to exceed the delay spread of the UWB channel and eliminate ISI, the relay is left with enough time for performing the amplifying and combining operations in (3) before the beginning of the second symbol duration. On the other hand, additional delays can be introduced to align the transmissions from the relays at integer multiples of T_s since the objective of the cooperation protocol is to produce distributed space-time codewords at D resulting in the discrete time index k rather than a continuous time variable. Given the fine temporal resolution of UWB systems and the fact that $\Delta_L + (M-1)\delta$ is small compared to T_s, aligning the signals received at D can be realized if the n-th relay delays its retransmission by τ_n which stands for the relative delay along the R$_n$-D link with respect to the direct link S-D. If this delay compensation is not carried out, the considered system model still holds with the sole modification of replacing the term $h_{n,n'}\left((m-m')\delta + \Delta_l\right)$ in (2) by $h_{n,n'}\left((m-m')\delta + \Delta_l + \tau_n\right)$ for $n' = N_r + 1$. In this case, the proposed scheme (in a way similar to the HD NAF scheme in [20]) can still achieve a full diversity order since only the elements of the channel matrices $H_{n,n'}$ will change without affecting the cooperation protocol and the corresponding STBC construction. In other words, unlike narrow-band systems, delay-tolerant STBC constructions as in [24] are not required for IR-UWB systems. Finally, note that, the time window $[\Delta_L + (M-1)\delta \quad T_s]$ that is large enough can be further exploited for mitigating the effects of loop interference at each relay. Loop interference cancelation in the UWB context falls beyond the scope of this work where the effects of the loop interference are embedded in the system design through the loop interference channels $H_{1,1}$ and $H_{2,2}$ and the magnitude terms $\rho_{1,1}$ and $\rho_{2,2}$. Finally, note that since the interference is eradicated at the symbol level, then the proposed scheme does not suffer from Inter-Block-Interference (IBI). In this context, the symbol duration is the same whether the cooperative solution is implemented or not given that multipath combining is performed at the relays. Combining this statement with the fact that the proposed ST codes transmit at the normalized rate of one symbol per channel use, then the proposed cooperative system does not suffer from any data-rate reductions compared to noncooperative systems.

B. Cooperation with One Relay

1) HD Relaying: The HD-NAF cooperation protocol in [3], [4], [20], [21] is presented as a benchmark. This protocol extends over four slots where the source transmits the symbols X_1, X_2, X_3 and X_4 sequentially during the four slots. $X_1, \ldots, X_4$ are M-dimensional vectors that correspond to encoded versions of some M-PPM information symbols carved from (1). In the HD operation mode, the relay is switched to receive in the first two slots (and hence it can not transmit) while the relay transmits amplified and combined versions of these received signals in the third and fourth slots. In other words, the signals transmitted by R$_1$ during the four slots are given by $X_1^{(1)} = 0_M$, $X_2^{(1)} = 0_M$, $X_3^{(1)} = \Psi_1 H_{0,1}^T Y_1^{(1)}$ and $X_4^{(1)} = \Psi_1 H_{0,1}^T Y_2^{(1)}$.

The signals received at R$_1$ and D are given by:

$$Y_k^{(1)} = \sqrt{P} H_{0,1} X_k + N_k^{(1)} \quad ; \quad k = 1, 2 \tag{4}$$

$$Z_k = \sqrt{P} H_{0,2} X_k + \sqrt{P} H_{1,2} X_k^{(1)} + N_k \quad ; \quad k = 1, \ldots, 4 \tag{5}$$

where P stands for the transmission level where we assume that the transmission levels from the source and relay(s) are the same over all slots and hence power allocation is not considered in this paper. $N_k^{(n)}$ stands for the LM-dimensional noise vector at the n-th relay during the k-th slot while N_k stands for the LM-dimensional noise vector at D during the k-th slot. $N_k^{(n)}$ and N_k are white Gaussian random vectors with autocorrelation $\frac{N_0}{2} I_{LM}$ where N_0 is the noise power spectral density.

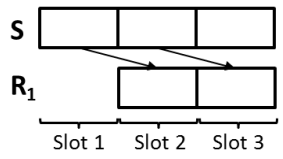

Fig. 3. One-relay cooperation protocol in the FD mode.

As will be explained later, the variable amplification matrix at R_1 is given by:

$$\Psi_1 = \left(H_{0,1}^T H_{0,1}\right)^{-\frac{1}{2}} \left(P H_{0,1}^T H_{0,1} + \frac{MN_0}{2} I_M\right)^{-\frac{1}{2}} \quad (6)$$

Equation (5) can be written as:

$$\mathcal{Z}_{(LM\times 4)}^{(\mathrm{HD},1)} = \mathcal{H}_{(LM\times 2M)}^{(\mathrm{HD},1)} \mathcal{X}_{(2M\times 4)}^{(\mathrm{HD},1)} + \mathcal{N}_{(LM\times 4)}^{(\mathrm{HD},1)} \quad (7)$$

where the subscripts indicate the corresponding matrices' dimensions. $\mathcal{N}^{(\mathrm{HD},1)}$ is a colored Gaussian noise vector, $\mathcal{Z}^{(\mathrm{HD},1)} = [Z_1, Z_2, Z_3, Z_4]$, $\mathcal{H}^{(\mathrm{HD},1)} = [\sqrt{P}H_{0,2} \quad P H_{1,2}\Psi_1 H_{0,1}^T H_{0,1}]$ and the distributed STBC is described by:

$$\mathcal{X}^{(\mathrm{HD},1)} = \begin{bmatrix} X_1 & X_2 & X_3 & X_4 \\ 0_M & 0_M & X_1 & X_2 \end{bmatrix} \quad (8)$$

Maximum Likelihood (ML) detection can be readily applied at D based on (7) after whitening the noise. In other words, the input of the decoder will consist of $\mathcal{Z}_w^{(\mathrm{HD},1)} = [Z_1, Z_2, \Sigma_1 Z_3, \Sigma_1 Z_4]$ that is corrupted by white noise where Σ_1 is the noise-whitening matrix given by:

$$\Sigma_1 = \left[I_{LM} + P(H_{1,2}\Psi_1 H_{0,1}^T)(H_{0,1}\Psi_1^T H_{1,2}^T)\right]^{-\frac{1}{2}} \quad (9)$$

2) FD Relaying: The reader is referred to Fig. 3. For $N_r = 1$, the cooperation strategy extends over three symbol durations or slots. (i): In the first slot, S transmits an encoded symbol denoted by the M-dimensional vector X_1. (ii): In the second slot, S proceeds with the transmission of a new encoded symbol X_2 while R_1 transmits the processed symbol $X_2^{(1)} = \Psi_1 H_{0,1}^T Y_1^{(1)}$. (iii): In the third slot, S transmits a new encoded symbol X_3 while R_1 transmits the symbol $X_3^{(1)} = \Psi_1 H_{0,1}^T Y_2^{(1)}$. Cooperation over three slots in the FD mode (rather than four slots in the HD mode) is now possible since in the second slot R_1 transmits $X_2^{(1)}$ while it receives $Y_2^{(1)}$ (that will be used for the generation of the subsequent symbol $X_3^{(1)}$) simultaneously.

The signals received at R_1 and D during the different slots can be written as:

$$Y_k^{(1)} = \sqrt{P}H_{0,1}X_k + \sqrt{P}H_{1,1}X_k^{(1)} + N_k^{(1)} \quad ; \quad k = 1,2,3 \quad (10)$$

$$Z_k = \sqrt{P}H_{0,2}X_k + \sqrt{P}H_{1,2}X_k^{(1)} + N_k \quad ; \quad k = 1,2,3 \quad (11)$$

where $X_1^{(1)} \triangleq 0_M$ since the relay is idle in the first slot. The second term in (10) stands for the self interference at the relay which constitutes a disadvantage compared to (4).

As shown in appendix A, the power of the signals retransmitted by the relay can be normalized by the following choice of the amplification matrix:

$$\Psi_1 = \left[H_{0,1}^T \left(P H_{0,1} H_{0,1}^T + P H_{1,1} H_{1,1}^T + \frac{MN_0}{2} I_{LM}\right) H_{0,1}\right]^{-\frac{1}{2}} \quad (12)$$

where removing the self-interference matrix $H_{1,1}$ results in the expression given in (6).

Replacing (10) recursively in (11) results in:

$$Z_1 = \sqrt{P}H_{0,2}X_1 + N_1 \quad (13)$$

$$Z_2 = \sqrt{P}H_{0,2}X_2 + P H_{1,2}\Psi_1 H_{0,1}^T H_{0,1} X_1 + \sqrt{P}H_{1,2}\Psi_1 H_{0,1}^T N_1^{(1)} + N_2 \quad (14)$$

$$Z_3 = \sqrt{P}H_{0,2}X_3 + P H_{1,2}\Psi_1 H_{0,1}^T H_{0,1} X_2 + P^{\frac{3}{2}} H_{1,2}\Psi_1 H_{0,1}^T H_{1,1}\Psi_1 H_{0,1}^T H_{0,1} X_1 + \sqrt{P}H_{1,2}\Psi_1 H_{0,1}^T N_2^{(1)} + P H_{1,2}\Psi_1 H_{0,1}^T H_{1,1}\Psi_1 H_{0,1}^T N_1^{(1)} + N_3 \quad (15)$$

Equations (13)-(15) can be written as:

$$\mathcal{Z}_{(LM\times 3)}^{(\mathrm{FD},1)} = \mathcal{H}_{(LM\times 3M)}^{(\mathrm{FD},1)} \mathcal{X}_{(3M\times 3)}^{(\mathrm{FD},1)} + \mathcal{N}_{(LM\times 3)}^{(\mathrm{FD},1)} \quad (16)$$

where $\mathcal{N}^{(\mathrm{FD},1)}$ is a colored Gaussian noise vector and $\mathcal{Z}^{(\mathrm{FD},1)} = [Z_1, Z_2, Z_3]$. The equivalent channel matrix is:

$$\mathcal{H}^{(\mathrm{FD},1)} = \left[\sqrt{P}H_{0,2} \quad P H_{1,2}\Psi_1 H_{0,1}^T H_{0,1} \quad P^{\frac{3}{2}} H_{1,2}\Psi_1 H_{0,1}^T H_{1,1}\Psi_1 H_{0,1}^T H_{0,1}\right] \quad (17)$$

The distributed FD-STBC is described by:

$$\mathcal{X}^{(\mathrm{FD},1)} = \begin{bmatrix} X_1 & X_2 & X_3 \\ 0_M & X_1 & X_2 \\ 0_M & 0_M & X_1 \end{bmatrix} \quad (18)$$

where the first row of $\mathcal{X}^{(\mathrm{FD},1)}$ represents the symbols transmitted by S, the second row represents the symbols transmitted by R_1 while the third row stands for the residual self interference where all previous symbols interfere with the current symbol. This is a particularity of the FD mode that did not appear in (8), for example.

Noise whitening can be realized by constructing the decision matrix $\mathcal{Z}_w^{(\mathrm{FD},1)} = [Z_1, \Sigma_1 Z_2, \Sigma_2 Z_3]$ where Σ_1 is given in (9) while Σ_2 takes the following form following from (15):

$$\Sigma_2 = \left[\Sigma_1^{-2} + P^2 (H_{1,2}\Psi_1 H_{0,1}^T)(H_{1,1}\Psi_1 H_{0,1}^T)(H_{0,1}\Psi_1^T H_{1,1}^T)(H_{0,1}\Psi_1^T H_{1,2}^T)\right]^{-\frac{1}{2}} \quad (19)$$

From (8) and (18), and in order to transmit the same power as non-cooperative systems, we set $P = \frac{4}{6} = \frac{2}{3}$ and $P = \frac{3}{5}$ for the HD mode and FD mode, respectively.

C. Cooperation with Two Relays

1) HD Relaying: For $N_r = 2$, the HD NAF protocol extends over eight slots and can be described by the following input-output relation:

$$\mathcal{Z}_{(LM\times 8)}^{(\mathrm{HD},2)} = \mathcal{H}_{(LM\times 3M)}^{(\mathrm{HD},2)} \mathcal{X}_{(3M\times 8)}^{(\mathrm{HD},2)} + \mathcal{N}_{(LM\times 8)}^{(\mathrm{HD},2)} \quad (20)$$

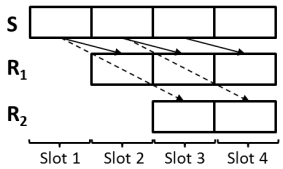

Fig. 4. Two-relay cooperation protocol in the FD mode.

where the equivalent channel matrix $\mathcal{H}^{(\mathrm{HD},2)}$ is given by: $\mathcal{H}^{(\mathrm{HD},2)} = [\sqrt{P}H_{0,3} \quad PH_{1,3}\Psi_1 H_{0,1}^T H_{0,1} \quad PH_{2,3}\Psi_2 H_{0,2}^T H_{0,2}]$ where Ψ_1 is given in (6) while $\Psi_2 = \left(H_{0,2}^T H_{0,2}\right)^{-\frac{1}{2}} \left(PH_{0,2}^T H_{0,2} + \frac{MN_0}{2} I_M\right)^{-\frac{1}{2}}$. $\mathcal{N}^{(\mathrm{HD},2)}$ is a colored Gaussian noise vector, $\mathcal{Z}^{(\mathrm{HD},2)} = [Z_1, \ldots, Z_8]$ and:

$$\mathcal{X}^{(\mathrm{HD},2)} = \begin{bmatrix} X_1 & X_2 & X_3 & X_4 & X_5 & X_6 & X_7 & X_8 \\ 0_M & 0_M & X_1 & X_2 & 0_M & 0_M & 0_M & 0_M \\ 0_M & 0_M & 0_M & 0_M & 0_M & 0_M & X_5 & X_6 \end{bmatrix} \quad (21)$$

where, imposed by the HD mode, R_1 receives in slots 1 and 2 and transmits in slots 3 and 4 while R_2 receives in slots 5 and 6 and transmits in slots 7 and 8. A decision matrix that is corrupted by white noise can be constructed as: $\mathcal{Z}_w^{(\mathrm{HD},2)} = [Z_1, Z_2, \Sigma_3 Z_3, \Sigma_3 Z_4, Z_5, Z_6, \Sigma_4 Z_7, \Sigma_4 Z_8]$ where $\Sigma_3 = \left[I_{LM} + P(H_{1,3}\Psi_1 H_{0,1}^T)(H_{0,1}\Psi_1^T H_{1,3}^T)\right]^{-\frac{1}{2}}$ and $\Sigma_4 = \left[I_{LM} + P(H_{2,3}\Psi_2 H_{0,2}^T)(H_{0,2}\Psi_2^T H_{2,3}^T)\right]^{-\frac{1}{2}}$.

2) FD Relaying: The reader is referred to Fig. 4. For $N_r = 2$, the cooperation strategy extends over four slots. The source transmits the encoded symbols X_1, X_2, X_3 and X_4 sequentially during the four slots. R_1 remains idle over the first slot while in the remaining slots it retransmits the signals it receives processed and delayed by one slot. In other words, R_1 transmits $X_1^{(1)} = 0_M$, $X_2^{(1)} = \Psi_1 H_{0,1}^T Y_1^{(1)}$, $X_3^{(1)} = \Psi_1 H_{0,1}^T Y_2^{(1)}$ and $X_4^{(1)} = \Psi_1 H_{0,1}^T Y_3^{(1)}$ in the four slots. In a similar way, R_2 remains idle over the first two slots and in the remaining slots it retransmits the signals it receives processed and delayed by two slots; that is, $X_1^{(2)} = 0$, $X_2^{(2)} = 0$, $X_3^{(2)} = \Psi_2 H_{0,2}^T Y_1^{(2)}$ and $X_4^{(2)} = \Psi_2 H_{0,2}^T Y_2^{(2)}$.

The signals received at R_1, R_2 and D can be written as ($k = 1, \ldots, 4$):

$$Y_k^{(1)} = \sqrt{P}H_{0,1}X_k + \sqrt{P}H_{1,1}X_k^{(1)} + \sqrt{P}H_{2,1}X_k^{(2)} + N_k^{(1)} \quad (22)$$

$$Y_k^{(2)} = \sqrt{P}H_{0,2}X_k + \sqrt{P}H_{1,2}X_k^{(1)} + \sqrt{P}H_{2,2}X_k^{(2)} + N_k^{(2)} \quad (23)$$

$$Z_k = \sqrt{P}H_{0,3}X_k + \sqrt{P}H_{1,3}X_k^{(1)} + \sqrt{P}H_{2,3}X_k^{(2)} + N_k \quad (24)$$

where, in addition to the self interference generated at each relay, the two relays interfere with each other since, unlike the NAF protocol, the relays are allowed to transmit at the same time.

Replacing $\{X_k^{(1)}, X_k^{(2)}\}_{k=1}^4$ by their values in (22)-(24), straightforward calculations show that the input-output relation of the relay-assisted FD system can be written as:

$$\mathcal{Z}_{(LM\times 4)}^{(\mathrm{FD},2)} = \mathcal{H}_{(LM\times 4M)}^{(\mathrm{FD},2)} \mathcal{X}_{(4M\times 4)}^{(\mathrm{FD},2)} + \mathcal{N}_{(LM\times 4)}^{(\mathrm{FD},2)} \quad (25)$$

where $\mathcal{N}^{(\mathrm{FD},2)}$ is a colored Gaussian noise vector and $\mathcal{Z}^{(\mathrm{FD},2)} = [Z_1, \ldots, Z_4]$.

The equivalent channel matrix is given by:

$$\mathcal{H}^{(\mathrm{FD},2)} = \Big[\sqrt{P}H_{0,3} \quad PU_1 H_{0,1} \quad PU_2 H_{0,2} + P^{\frac{3}{2}} U_1 U_3 H_{0,1} \quad P^2 U_1 U_3^2 H_{0,1} + P^{\frac{3}{2}}(U_2 U_4 H_{0,1} + U_1 U_5 H_{0,2})\Big] \quad (26)$$

where the matrices $U_1, \ldots, U_5$ are defined as follows:

$$U_1 = H_{1,3}\Psi_1 H_{0,1}^T \; ; \; U_2 = H_{2,3}\Psi_2 H_{0,2}^T \; ; \; U_3 = H_{1,1}\Psi_1 H_{0,1}^T$$
$$U_4 = H_{1,2}\Psi_1 H_{0,1}^T \; ; \; U_5 = H_{2,1}\Psi_2 H_{0,2}^T \quad (27)$$

The distributed STBC codewords take the following form:

$$\mathcal{X}^{(\mathrm{FD},2)} = \begin{bmatrix} X_1 & X_2 & X_3 & X_4 \\ 0_M & X_1 & X_2 & X_3 \\ 0_M & 0_M & X_1 & X_2 \\ 0_M & 0_M & 0_M & X_1 \end{bmatrix} \quad (28)$$

In this case of $N_r = 2$, the amplification matrices at the relays are given by:

$$\Psi_1 = \Big[H_{0,1}^T \Big(PH_{0,1}H_{0,1}^T + PH_{1,1}H_{1,1}^T + PH_{2,1}H_{2,1}^T + \frac{MN_0}{2} I_{LM}\Big) H_{0,1}\Big]^{-\frac{1}{2}} \quad (29)$$

$$\Psi_2 = \Big[H_{0,2}^T \Big(PH_{0,2}H_{0,2}^T + PH_{2,2}H_{2,2}^T + PH_{1,2}H_{1,2}^T + \frac{MN_0}{2} I_{LM}\Big) H_{0,2}\Big]^{-\frac{1}{2}} \quad (30)$$

where the proof is similar to that provided in appendix A.

Noise-whitening can be realized by constructing $\mathcal{Z}_w^{(\mathrm{FD},2)} = [Z_1, \Sigma_5 Z_2, \Sigma_6 Z_3, \Sigma_7 Z_4]$ where:

$$\Sigma_5 = \left[I_{LM} + PU_1 U_1^T\right]^{-\frac{1}{2}} \quad (31)$$

$$\Sigma_6 = \left[\Sigma_5^{-2} + PU_2 U_2^T + P^2 (U_1 U_3)(U_1 U_3)^T\right]^{-\frac{1}{2}} \quad (32)$$

$$\Sigma_7 = \Big[\Sigma_6^{-2} + P^2 (U_1 U_5)(U_1 U_5)^T + \left(P^3 U_1 U_3^2 + P^2 U_2 U_4\right)\left(P^3 U_1 U_3^2 + P^2 U_2 U_4\right)^T\Big]^{-\frac{1}{2}} \quad (33)$$

The transmit power can be normalized by setting $P = \frac{8}{12} = \frac{2}{3}$ and $P = \frac{4}{9}$ for the HD and FD modes following from (21) and (28), respectively.

Note that in the FD mode the relays are always receiving where $k = 1, 2, 3$ in (10) and $k = 1, \ldots, 4$ in (22)-(23). In the HD mode, R_1 is switched to receive in the first two slots ($k = 1, 2$ in (4)) while R_2 is switched to receive in slots $k = 3, 4$. Evidently, D is switched to receive over the entire span of the distributed ST codewords whether in the HD or FD modes.

Finally, it is worth noting that the implementation of the considered HD and FD cooperation schemes requires full channel state information (CSI) at the destination and the relays. In this context, operating in the FD mode does not induce any additional implications in terms of the complexity of the procedure for extracting the values of L path gains from the UWB channel impulse response. The additional complexity of the FD scheme resides in the need for estimating a larger number of channels since the self and inter-relay

interference-channels need to be estimated. In this context, for 1-relay systems, the number of estimated channels increases from 3 in the HD mode to 4 in the FD mode while for 2-relay systems this number increases from 5 to 9. Finally, for decoding the M-PPM symbols at D, the M-dimensional extension of the sphere decoder in [25] can be applied, for example.

III. Distributed Space-Time Codes

A. Code Construction

Designing nonorthogonal FD codes with N_r relays calls for embedding N_r+2 encoded symbols $X_1,\ldots,X_{N_r+2}$ (each being a distinct function of the N_r+2 information symbols $s_1,\ldots,s_{N_r+2}$) in the codewords that have the structure given in (18) and (28). Designing such encoded symbols in a manner that ensures a full diversity order turns out to be a challenging task. In this work, we present adhoc constructions with one relay and two relays. We hope that this work will motivate more research in the direction of systematic designs of FD codes with more than two relays.

1) One Relay: For $N_r=1$, (8) shows that four information symbols (carved from $\mathcal{C}$ in (1)) must be included in the encoded symbols $X_1,\ldots,X_4$ for the HD protocol to transmit at the same data rate as non-cooperative systems. In particular, the best known totally-real distributed HD-STBCs for PPM in [20], [21] are based on an algebraic construction and correspond to imposing the following structure on the codewords (the last two columns of $\mathcal{X}^{(\mathrm{HD},1)}$ in (8) where the simultaneous transmissions from S and R_1 occur):

$$C^{(\mathrm{HD},1)}(s_1,s_2,s_3,s_4)= \begin{bmatrix} X_3 & X_4 \\ X_1 & X_2 \end{bmatrix} = \begin{bmatrix} s_1+\phi s_2 & s_3+\phi s_4 \\ \Omega(s_3+\phi_1 s_4) & s_1+\phi_1 s_2 \end{bmatrix} \quad (34)$$

where $\phi=\frac{1+\sqrt{5}}{2}$ and $\phi_1=\frac{1-\sqrt{5}}{2}$ are the golden number and its conjugate, respectively. Ω is a $M\times M$ matrix given by $\Omega=\begin{bmatrix} 0 & 1 \\ -1 & 0 \end{bmatrix}$ for $M=2$ [21] and by the following expression of $M>2$ [20] ($0_{m\times n}$ is the $m\times n$ all-zero matrix):

$$\Omega=\begin{bmatrix} 0_{1\times(M-1)} & 1 \\ I_{M-1} & 0_{(M-1)\times 1} \end{bmatrix} \quad (35)$$

The biggest advantage of the FD operation mode over the HD mode resides in the fact that only three information symbols need to be incorporated in the STBC codewords as shown in (18). This results in a reduced decoding complexity where the total number of information vectors is reduced from M^4 to M^3. This also offers the possibility of achieving higher coding gains as will be highlighted later. On the other hand, the structure of the codewords is imposed by the FD protocol which renders the systematic algebraic-based constructions inappropriate for this class of FD-STBCs. From (18), the simultaneous transmissions from S and R_1 occur over the second and third slots and the distributed STBC codewords must respect the following structure $\begin{bmatrix} X_2 & X_3 \\ X_1 & X_2 \end{bmatrix}$ where the two M-dimensional diagonal vectors must be equal. In order to achieve a full diversity order with enhanced coding gains, we propose the following STBC scheme:

$$C^{(\mathrm{FD},1)}(s_1,s_2,s_3)=\begin{bmatrix} X_2 & X_3 \\ X_1 & X_2 \end{bmatrix}=\begin{bmatrix} s_1 & s_2+\Gamma s_3 \\ \Omega(s_2+\Gamma s_3) & s_1 \end{bmatrix} \quad (36)$$

where $s_1,\ldots,s_3\in\mathcal{C}$ in (1), Ω is given in (35) for all values of M and Γ is a $M\times M$ unitary matrix that takes the following form with 2-PPM:

$$\Gamma=\begin{bmatrix} 0 & 1 \\ -1 & 0 \end{bmatrix} \quad ; \quad M=2 \quad (37)$$

and the following form with M-PPM where $M>2$ and even:

$$\Gamma=I_{M/2}\otimes\frac{1}{\sqrt{2}}\begin{bmatrix} 1 & 1 \\ -1 & 1 \end{bmatrix} \quad ; \quad M>2 \ , \ M \text{ even} \quad (38)$$

where $\otimes$ stands for the Kronecker product.

2) Two Relays: For $N_r=2$, (21) shows that HD-STBCs comprise the joint encoding/decoding of eight information symbols which constitutes the approach adopted in [4], [20], [21]. In a way similar to the complex constructions in [4], the best-known real constructions in [20], [21] are based on the following choice of the codewords (columns 3, 4, 7 and 8 of $\mathcal{X}^{(\mathrm{HD},2)}$ in (21) where the simultaneous transmissions from S and either R_1 or R_2 occur):

$$C^{(\mathrm{HD},2)}(s_1,\ldots,s_8)=\begin{bmatrix} X_3 & X_4 & X_7 & X_8 \\ X_1 & X_2 & 0_M & 0_M \\ 0_M & 0_M & X_5 & X_6 \end{bmatrix} \quad (39)$$

where $X_3=s_1+\theta s_2+\phi(s_3+\theta s_4)$ and $X_4=s_5+\theta s_6+\phi(s_7+\theta s_8)$. In this case, $X_2=\sigma(X_3)$ and $X_1=\Omega\sigma(X_4)$ where $\sigma(.)$ corresponds to replacing $\phi=\frac{1+\sqrt{5}}{2}$ by $\phi_1=\frac{1-\sqrt{5}}{2}$ and Ω is as defined in the case $N_r=1$. Finally, $X_7=\tau(X_3)$, $X_8=\tau(X_4)$, $X_5=\tau(X_1)$ and $X_6=\tau(X_2)$ where $\tau(.)$ corresponds to replacing $\theta=1+\sqrt{2}$ by $\theta_1=1-\sqrt{2}$ [20], [21].

In the FD operation mode, following from (28) that imposes the structure of the codewords, we propose the following encoding scheme:

$$C^{(\mathrm{FD},2)}(s_1,s_2,s_3,s_4)= \begin{bmatrix} X_2 & X_3 & X_4 \\ X_1 & X_2 & X_3 \\ 0_M & X_1 & X_2 \end{bmatrix}=\begin{bmatrix} s_3+\Gamma s_4 & s_2 & s_1+\Gamma s_3 \\ s_1+\Gamma s_2 & s_3+\Gamma s_4 & s_2 \\ 0_M & s_1+\Gamma s_2 & s_3+\Gamma s_4 \end{bmatrix} \quad (40)$$

where it is now sufficient to incorporate four symbols in each codeword rather than eight symbols as in (39). Γ is given in (37) for $M=2$ and in (38) for $M>2$ and even, respectively.

B. Diversity Order

The diversity order is defined as the minimum rank of the difference between any two non-identical codewords [26]. We will next prove that the codewords in (36) (resp. (40)) achieve the full diversity order of $d=2$ (resp. $d=3$) in the case of one relay (resp. two relays). Note that unlike the case of Rayleigh fading channels where a diversity order of d implies that the error rates will scale asymptotically as SNR^{-d}, analogous relations do not hold over the more involved IEEE 802.15.3a

channel model [27], [28]. For an arbitrary channel model, d is equal to the number of independent parallel links between the source and destination and is at most equal to $N_r + 1$ following from the presence of the links S-D, S-R_1-D, ..., S-R_{N_r}-D between S and D. In this case, the transmitted message can be reconstructed at D if any $d-1$ (or less) paths among S-D, S-R_1, ..., S-R_{N_r}, R_1-D, ..., R_{N_r}-D suffer from severe fading simultaneously.

Based on the rank criterion [26], the proposed codes achieve a full diversity order if the matrix $C^{(\mathrm{FD},N_r)}(a_1,\ldots,a_{N_r+2})$ has a full rank of N_r+1 for $(a_1,\ldots,a_{N_r+2}) \in \mathcal{A}^{N_r+2}\backslash\{(0_M,\ldots,0_M)\}$ where $\mathcal{A}$ denotes the set of all possible differences between two information vectors:

$$\mathcal{A} = \{s - s' \ ; \ s, s' \in \mathcal{C}\} \tag{41}$$

From (1), elements of $\mathcal{A}$ are either equal to 0_M or have exactly two nonzero components with one of them equal to $+1$ while the other one equal to -1. The transmit diversity is achieved because of this particular structure of $\mathcal{A}$. For example, the matrix $C^{(\mathrm{FD},1)}(a_1,a_2,a_3)$ is rank-deficient when $a_3 = 0_M$ and $a_1 = a_2 = 1_M$ where 1_M is the M-dimensional vector having all of its components equal to 1. However, 1_M is not an element of $\mathcal{A}$ for all values of M.

The choice of the matrix Γ as in (37) and (38) allows to satisfy the following two properties that are crucial for proving that the proposed codes are fully diverse with $N_r = 1$ and $N_r = 2$.

Property 1: For any two elements a_1 and a_2 of $\mathcal{A}$, $a_1 + \Gamma a_2 = 0_M$ if and only if $a_1 = a_2 = 0_M$.

Proof: For $M = 2$, $a_1 \in \mathcal{A} = \{[0\ 0]^T, \pm[-1\ 1]^T\}$ while $a_2' \triangleq \Gamma a_2 \in \mathcal{A}' \triangleq \{\Gamma a \ ; \ a \in \mathcal{A}\} = \{[0\ 0]^T, \pm[1\ 1]^T\}$ which directly proves property 1.

For $M > 2$ and even, consider a nonzero vector a_2 of $\mathcal{A}$ and denote its two nonzero components by a_{2,m_1} and a_{2,m_2} where $m_1 < m_2$ for convenience. The structure of the set $\mathcal{A}$ implies that $a_{2,m_1} \in \{\pm 1\}$ and $a_{2,m_2} = -a_{2,m_1}$. Two cases need to be considered following from (38). Case (i): m_1 odd and $m_2 = m_1 + 1$. In this case, $a_2' \triangleq \Gamma a_2$ has all of its components equal to zero except for its m_2-th component $a'_{2,m_2} = \pm\frac{2}{\sqrt{2}}$. Case (ii): for m_1 and m_2 not satisfying the conditions in case (i). In this case, a_2' will have four nonzero components that extend over the positions m_1, $\pi(m_1)$, m_2 and $\pi(m_2)$ where $\pi(m) = m+1$ if m is odd and $\pi(m) = m-1$ if m is even. Moreover, the values of these nonzero components are not arbitrary and are limited to $(a'_{2,m_1}, a'_{2,\pi(m_1)}, a'_{2,m_2}, a'_{2,\pi(m_2)}) \in \frac{1}{\sqrt{2}}\{\pm(1,1,-1,-1), \pm(1,1,-1,1)\}, \pm(1,-1,-1,1), \pm(1,-1,1,1)\}$. In both of the above cases, a_2' can not be equal to a nonzero element of $\mathcal{A}$ that has exactly two nonzero components. Consequently, the relation $a_1 + \Gamma a_2 = 0_M$ implies that $a_2' = -a_1 \in \mathcal{A}$ (since $-\mathcal{A} = \mathcal{A}$) implying that $a_2' = 0_M$ since nonzero values of a_2' can not be equal to an element of $\mathcal{A}$ as proven above. Now, $a_2' = 0_M$ implies that $a_2 = 0_M$ and $a_1 = 0_M$ completing the proof of property 1. ∎

Property 2: For any three elements a_1, a_2 and a_3 of $\mathcal{A}$, $a_1 + \Gamma a_2 = r a_3$ if and only if $a_2 = 0_M$ where r is any nonzero real number.

Proof: If $a_3 = 0_M$, then property 2 reduces to property 1 implying that $a_1 = a_2 = 0_M$. Therefore, we next consider the case $a_3 \neq 0_M$.

For $M = 2$, $a_1 + \Gamma a_2 \in \{[0\ 0]^T, \pm[-1\ 1]^T, \pm[1\ 1]^T, \pm[2\ 0]^T, \pm[0\ 2]^T\}$. The only nonzero vectors of this set that can be proportional to a nonzero element of $\mathcal{A}$ are $\pm[-1\ 1]^T$. However, these two elements result uniquely from $a_1 \in \{\pm[-1\ 1]^T\}$ and $a_2 = 0_M$ proving property 2.

For $M > 2$ and even, assume that $a_2' = \Gamma a_2 \neq 0_M$. From the two cases considered in the proof of property 1, a_2' can have one or four nonzero components. Consequently, $a_1 + a_2'$ will have one or four nonzero components if $a_1 = 0_M$ while this vector will have between two and six nonzero components if $a_1 \neq 0_M$ since nonzero elements of $\mathcal{A}$ have exactly two nonzero components. For $a_1 + a_2'$ to be proportional to a nonzero element $a_3 \in \mathcal{A}$ having two nonzero components, this vector must itself have exactly two nonzero components. From the properties of the sets $\mathcal{A}$ and $\mathcal{A}' = \Gamma\mathcal{A}$, this case arises only when a_2' has one nonzero component whose position coincides with one of the positions of the nonzero components of a_1. In other words, the pair of nonzero components of $a_1 + a_2'$ can be either equal to $(1 \pm \frac{2}{\sqrt{2}}, -1)$ or $(-1 \pm \frac{2}{\sqrt{2}}, 1)$ implying that this vector can not be proportional to a_3 whose two nonzero components take the values $\pm(1,-1)$. Therefore, $a_2' = 0_M$ and $a_2 = 0_M$ completing the proof. ∎

Proposition 1: The proposed distributed STBC in (36) achieves full transmit diversity with $N_r = 1$ relay and M-PPM for all even values of M.

Proof: We will prove that the proposed code is fully-diverse by proving that the matrix $C^{(\mathrm{FD},1)}(a_1,a_2,a_3)$ in (36) is rank-deficient only when $a_1 = a_2 = a_3 = 0_M$. This matrix will be referred to as C when there is no ambiguity. $\mathrm{rank}(C) < 2$ if $r_1 C_1 + r_2 C_2 = 0_{2M}$ where C_i is the i-th column of C and r_1 and r_2 are two real numbers satisfying $(r_1, r_2) \neq (0,0)$. From (36) this implies that:

$$r_1 a_1 + r_2(a_2 + \Gamma a_3) = 0_M \tag{42}$$

$$r_1 \Omega(a_2 + \Gamma a_3) + r_2 a_1 = 0_M \tag{43}$$

The following three cases arise. Case 1: $r_1 = 0$ and $r_2 \neq 0$. In this case, (43) results in $a_1 = 0_M$ while (42) results in $a_2 + \Gamma a_3 = 0_M$ implying that $a_2 = a_3 = 0_M$ from property 1. Case 2: $r_1 \neq 0$ and $r_2 = 0$. In this case, (42) results in $a_1 = 0_M$. On the other hand, (43) results in $\Omega(a_2 + \Gamma a_3) = 0_M$ which implies that $a_2 + \Gamma a_3 = 0_M$ resulting in $a_2 = a_3 = 0_M$ from property 1. Case 3: $r_1 \neq 0$ and $r_2 \neq 0$. In this case, (42) implies that $a_2 + \Gamma a_3 = -\frac{r_1}{r_2} a_1$ which implies that $a_3 = 0_M$ from property 2 since $-\frac{r_1}{r_2} \neq 0$. Setting $a_3 = 0_M$ in (42) and (43) results in $a_1 = -\frac{r_2}{r_1} a_2$ and $\Omega a_2 = -\frac{r_2}{r_1} a_1$, respectively. These equations can be combined as $\Omega a_2 = \left(\frac{r_2}{r_1}\right)^2 a_2$ which shows that a_2 is an eigenvector of the matrix Ω associated with the positive real eigenvalue $\left(\frac{r_2}{r_1}\right)^2$. Following from the structure of the permutation matrix Ω in (35), its eigenvalues are given by the roots of unity $e^{\frac{2\pi m i}{M}}$ for $m = 0, \ldots, M-1$. The only positive real eigenvalue is equal to 1 and the corresponding eigenvector has all of its components equal to

each other implying that it can not be equal to a nonzero element of $\mathcal{A}$. In other words, over the set $\mathcal{A}$, the equation $\Omega a_2 = \left(\frac{r_2}{r_1}\right)^2 a_2$ admits only the trivial solution $a_2 = 0_M$. Finally, replacing $a_3 = 0_M$ and $a_2 = 0_M$ in either (42) or (43) results in $a_1 = 0_M$. As a conclusion, the above three cases show that the only rank-deficient matrix is the $2M \times 2$ all-zero matrix that results from $a_1 = a_2 = a_3 = 0_M$ implying that the proposed code is fully diverse. ■

Proposition 2: The proposed distributed STBC in (40) achieves full transmit diversity with $N_r = 2$ relays and M-PPM for all even values of M.

Proof: The proof is based on the same concept as in the case $N_r = 1$, yet it is more involved. This proof is provided in appendix B. ■

C. Comparison between the FD-STBCs and HD-STBCs

For $N_r = 1$, we define the minimum determinant as $\delta_{min}(M) = \min_{C \neq 0_{2M\times 2}}[\det(C^T C)]^{1/2}$ for a certain value of M. For the HD-STBC, $\delta_{min}(M) = \frac{2}{\sqrt{5}} = 0.8944$ for all values of M [20], [21] which is the same as for the complex-valued construction in [4]. In this context, the proposed STBC in the FD mode is characterized by $\delta_{min}(2) = 2$ and $\delta_{min}(M) = 2(2 - \sqrt{2}) = 1.1716$ for $M > 2$ (and even). Note that the last value was determined by evaluating $\delta_{min}(4) = 1.1716$ numerically and by observing that increasing M increases the number of dimensions and hence does not affect the minimum determinant [20].

Note that, inspired from the HD-STBC in (34), a feasible alternative to the FD-STBC in (36) would be:

$$C(s_1, s_2, s_3) = \begin{bmatrix} X_2 & X_3 \\ X_1 & X_2 \end{bmatrix} = \begin{bmatrix} s_1 & s_2 + \phi s_3 \\ \Omega(s_2 + \phi_1 s_3) & s_1 \end{bmatrix} \tag{44}$$

however, the achievable minimum determinant would be the same as in the HD mode ($\delta_{min}(M) = 0.8944$) thus highlighting the advantage of the proposed FD-STBC.

For $N_r = 2$ with M-PPM, we define the minimum determinant as $\delta_{min}(M) = \min_{C \neq \mathbf{0}}[\det(C^T C)]^{1/3}$ where $\mathbf{0} = 0_{3M\times 4}$ for the HD mode and $\mathbf{0} = 0_{3M\times 3}$ for the FD mode. For the HD-STBC, $\delta_{min}(M) = 0.4642$ for all values of M [20], [21] where in this case the totally-real constraint reduced the minimum determinant compared to the complex construction in [4]. On the other hand, for the FD-STBC, $\delta_{min}(2) = 2$ and $\delta_{min}(M) = 1.262$ for $M > 2$.

Comparing the FD-STBCs and HD-STBCs. (i): Both codes are totally-real, fully-diverse and do not introduce any data-rate reductions compared to non-cooperative systems. (ii): The FD mode benefits from higher coding gains (larger δ_{min}) especially with 2-PPM; this helps in compensating for the detrimental effect of self-interference and will result in enhanced performance levels as will be highlighted in the next section. (iii): The FD-STBC is associated with a reduced decoding complexity where three (resp. four) symbols, rather than four (resp. eight) symbols, need to be jointly decoded for $N_r = 1$ (resp. $N_r = 2$). (iv): Compared to the HD mode, the FD mode presents the additional advantages of lower decoding delays and lower peak-to-average power ratios (PAPR). In particular, for $N_r = 1$, the decoding delay decreases from four symbol durations to three symbol durations while the PAPR decreases by 4.51 dB and 2 dB for $M = 2$ and $M > 2$, respectively. On the other hand, for $N_r = 2$, the decoding delay decreases from eight symbol durations to four symbol durations while the PAPR decreases by 6.94 dB for $M = 2$ and 4.61 dB for $M > 2$.

IV. Numerical Results

The UWB channels between the different nodes are generated independently according to the IEEE 802.15.3a NLOS channel model recommendation CM2 [22]. As indicated above, the LOS channel model recommendation CM1 is adopted for generating the self-interference channel between the transmit and receive antennas of the same relay. A Gaussian pulse with a duration of $T_w = 0.5$ ns is used and the modulation delay is set to $\delta = 0.5$ ns. In order to eliminate the ISI, the symbol duration is set to $T_s = 100$ ns. The delay of the l-th Rake finger is chosen as $\Delta_l = (l-1)MT_w$ for $l = 1, \ldots, L$. The channel is held constant over one transmission block, and is allowed to change independently from one block to another. Perfect CSI is assumed at the destination and the relays and the ML PPM decoder in [25] is applied. The presented results show the symbol error rates (SER) as a function of the SNR per information bit where the SER was numerically averaged over $10,000$ randomly generated channels. The received SNR per information bit is defined as $\frac{1}{N_0 \log_2 M}$ where the average power of the M-PPM constellations was normalized to unity. Finally, we set $\rho_{n,n} = 1$ for $n = 1, 2$. As has been highlighted in subsection II.A, this corresponds to the extreme case scenario where the residual self loop interference does not decrease with the SNR and assumes its maximum practical value of 1. The presented results show that the proposed FD scheme achievers higher performance levels compared to the HD scheme in this scenario and, consequently, they demonstrate the superiority of the former under all practical network and interference conditions.

Fig. 5 shows the performance of 2-PPM with one relay. The distances source-relay, relay-destination and source-destination are taken to be the same resulting in $\rho_{0,1} = \rho_{1,2} = 1$. Results show the superiority of the FD-STBC compared to the HD-STBC in [21] despite the residual self loop interference. The proposed family of codes in the FD mode ensures a full transmit diversity order as the HD-STBC and the corresponding error curves are practically parallel for large values of the SNR. The slopes of these curves are also enhanced compared to the case of non-cooperative transmissions. In other words, the proposed encoding scheme not only eliminates the error floors that are often associated with the FD mode, but also profits from the same diversity order that can be achieved in the simplistic HD mode. Finally, as indicated in subsection III-C, it is worth noting that the performance gains of the FD-STBC are associated with simplified decoding

Fig. 6 shows the performance of M-PPM with one relay for various values of M. A 1-finger Rake is used and we fix $\rho_{0,1} = \rho_{1,2} = 1$ for 2-PPM and 4-PPM and $\rho_{0,1} = \rho_{1,2} = 4$ (the relay is half-way between S and D with a pathloss

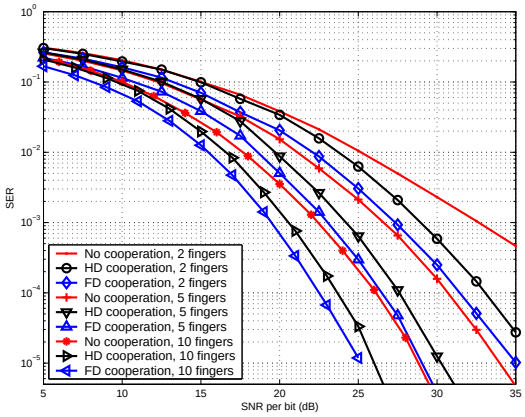

Fig. 5. Performance of 2-PPM with 1 relay and $\rho_{0,1} = \rho_{1,2} = 1$.

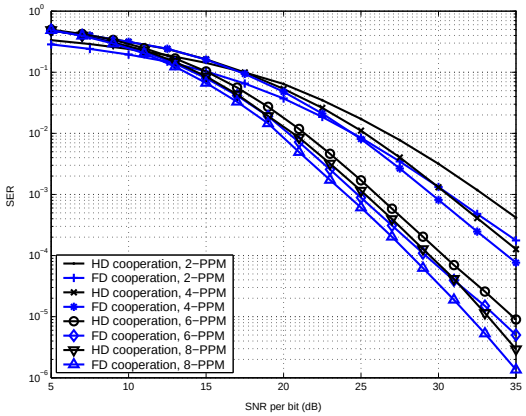

Fig. 6. Performance with 1 relay and a 1-finger Rake. $\rho_{0,1} = \rho_{1,2} = 1$ for 2-PPM and 4-PPM while $\rho_{0,1} = \rho_{1,2} = 4$ for 6-PPM and 8-PPM.

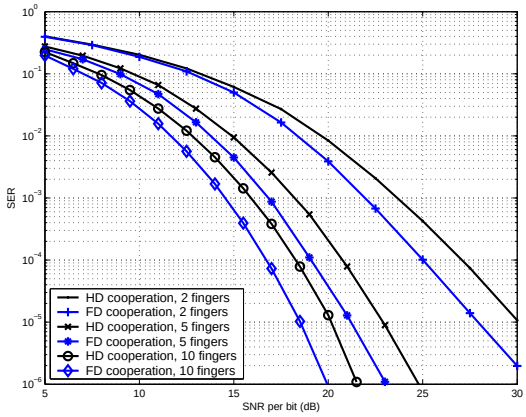

Fig. 7. Performance of 4-PPM with 2 relays. $\rho_{0,1} = \rho_{0,2} = 4$, $\rho_{1,3} = \rho_{2,3} = 1$ and $\rho_{1,2} = \rho_{2,1} = 1$.

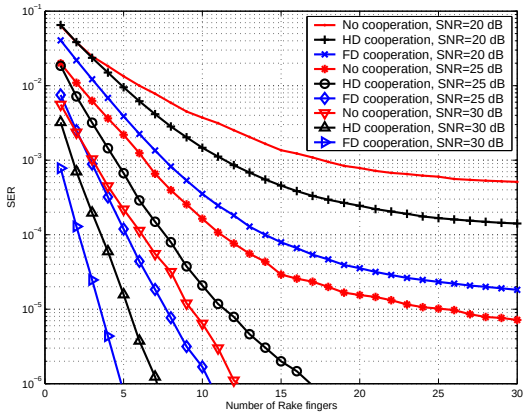

Fig. 8. Performance of 2-PPM with 2 relays. $\rho_{0,1} = \rho_{0,2} = \rho_{1,3} = \rho_{2,3} = 1$ and $\rho_{1,2} = \rho_{2,1} = 1$.

exponent of 2) for 6-PPM and 8-PPM. Results show the superiority of the proposed FD-STBC with different modulation formats. As expected, the highest performance enhancements are observed with 2-PPM for which the coding gain of the proposed code is the highest. In this case, operating in the FD mode results in a performance gain of about 2.2 dB at 10^{-3}. Comparing the different modulation schemes shows that M-PPM constellations with larger values of M are capable of achieving better performance levels at larger SNRs in coherence with [29].

Fig. 7 shows the performance of 4-PPM with two relays. The two relays occupy symmetrical positions that are closer to S with $\rho_{0,1} = \rho_{0,2} = 4$ and $\rho_{1,3} = \rho_{2,3} = 1$. The interference between the two relays is adjusted by setting $\rho_{1,2} = \rho_{2,1} = 1$. Results show that, as in the case of one relay, the proposed FD-STBC is fully-diverse and achieves the same full diversity order as the HD-STBC in [20] with two relays. Despite the excessive levels of interference in the FD mode, a smaller number of symbols need to be inserted in each codeword resulting in performance gains in the order of 1.7 dB, 1.4 dB and 1.4 dB with $L = 2$, 5 and 10, respectively. These performance gains are associated with a reduced decoding complexity. For example, with $L = 5$ and at a SNR of 10 dB, the decoder in [25] converges around 5.5 times faster with the FD-STBC compared to the HD-STBC.

Fig. 8 shows the impact of the number of Rake fingers on the performance of HD and FD cooperative systems as well as noncooperative systems. Simulations are performed with two relays, 2-PPM, $\rho_{0,1} = \rho_{0,2} = \rho_{1,3} = \rho_{2,3} = 1$ and $\rho_{1,2} = \rho_{2,1} = 1$. The superiority of the proposed FD-STBC is evident with any number of Rake fingers. This figure highlights the usefulness of spatial diversity even in UWB systems that profit from rich multi-path diversity. In fact, at a given SNR, increasing the number of Rake fingers L (number of combined multi-path components) does not always enhance the performance where error floors manifest for large values of L. This follows mainly from the high correlation between the different multi-path components [22] and from the fact that more noise is integrated in the receiver when L increases. In this context, taking advantage of the spatial diversity through distributed schemes allows to reduce these error floors and achieve improved performance levels with an acceptable number of Rake fingers.

V. Conclusion

In this paper, we investigated the advantages of FD relaying in the context of IR-UWB communications. We examined the implications of the FD operation mode on the space-time code design and proposed accordingly two novel STBC

constructions that are appropriate for PPM with one and two relays. The FD operation mode adds new degrees of freedom to the problem of STBC design capable of leveraging the critical effects of self loop interference. We hope that this work will motivate future research in this direction and in investigating loop interference mitigating techniques in the context of UWB.

APPENDIX A

For the PPM symbols $\{X_k\}$ that can be equal to any column of the identity matrix I_M:

$$\mathrm{E}[X_k X_k^T] = \frac{1}{M} I_M \tag{45}$$

and the PPM constellation has an average power that is normalized to unity: $\mathrm{Tr}\left[\mathrm{E}[X_k X_k^T]\right] = 1$.

The same structure of the covariance matrix in (45) will be imposed on the symbols $\{X_k^{(1)}\}$ retransmitted by the relay. The power constraint at the relay can be expressed as: $\mathrm{E}\left[\mathrm{Tr}\left[X_k^{(1)}[X_k^{(1)}]^T\right]\right] = 1$ which from (3) and (10) results in:

$$\mathrm{Tr}\left[\Psi_1 H_{0,1}^T \mathrm{E}\left[\left(\sqrt{P}H_{0,1}X_k + \sqrt{P}H_{1,1}X_k^{(1)} + N_k^{(1)}\right)\times \left(\sqrt{P}X_k^T H_{0,1}^T + \sqrt{P}[X_k^{(1)}]^T H_{1,1}^T + [N_k^{(1)}]^T\right)\right] H_{0,1}\Psi_1^T\right] = 1 \tag{46}$$

which implies that:

$$\mathrm{Tr}\left[\Psi_1^T \Psi_1 H_{0,1}^T \left(\frac{P}{M} H_{0,1} H_{0,1}^T + \frac{P}{M} H_{1,1} H_{1,1}^T + \frac{N_0}{2} I_{LM}\right) H_{0,1}\right] = 1 \tag{47}$$

where the last equation follows from (i): the conditions on the covariance matrices $\mathrm{E}\left[X_k X_k^T\right] = \mathrm{E}\left[X_k^{(1)}[X_k^{(1)}]^T\right] = \frac{1}{M} I_M$. (ii): the fact that the noise is zero-mean with covariance matrix $\frac{N_0}{2} I_{LM}$ and (iii): the fact that X_k (the current symbol transmitted by the source) and the symbol $X_k^{(1)}$ (the current symbol transmitted by the relay that depends on the previous symbols transmitted by the source) are independent. The relation $\mathrm{Tr}[AB] = \mathrm{Tr}[BA]$ was also invoked in (47).

A solution for (47) can be obtained by choosing Ψ_1 to be a symmetrical matrix satisfying $\Psi_1^2 \left[H_{0,1}^T \left(\frac{P}{M} H_{0,1} H_{0,1}^T + \frac{P}{M} H_{1,1} H_{1,1}^T + \frac{N_0}{2} I_{LM}\right) H_{0,1}\right] = \frac{1}{M} I_M$ which implies that the condition on the covariance matrix of $X_k^{(1)}$ is satisfied. The solution of this equation results in (12).

APPENDIX B

The matrix $C^{(\mathrm{FD},2)}(a_1, \ldots, a_4)$ in (40) will be referred to as C when there is no ambiguity. $\mathrm{rank}(C) < 3$ if there exist three real numbers $(r_1, r_2, r_3) \neq (0,0,0)$ such that $\sum_{i=1}^{3} r_i C_i = 0_{3M}$ where C_i is the i-th column of C. From (40), this results in the following three equalities:

$$r_1(a_3 + \Gamma a_4) + r_2 a_2 + r_3(a_1 + \Gamma a_3) = 0_M \tag{48}$$

$$r_1(a_1 + \Gamma a_2) + r_2(a_3 + \Gamma a_4) + r_3 a_2 = 0_M \tag{49}$$

$$r_2(a_1 + \Gamma a_2) + r_3(a_3 + \Gamma a_4) = 0_M \tag{50}$$

We will next prove that the only solution to the above equations over the set $\mathcal{A}$ is given by $(a_1, a_2, a_3, a_4) = (0_M, 0_M, 0_M, 0_M)$. The following cases need to be considered separately. Case 1: $r_1 = r_2 = 0$ and $r_3 \neq 0$. In this case, (49) implies that $a_2 = 0_M$ while (48) and (50) result in $a_1 = a_3 = a_4 = 0_M$ following from property 1. Case 2: $r_1 = r_3 = 0$ and $r_2 \neq 0$. In this case, (48) results in $a_2 = 0_M$. Replacing $a_2 = 0_M$ in (50) results in $a_1 = 0_M$. Finally, (49) results in $a_3 = a_4 = 0_M$ from property 1. Case 3: $r_2 = r_3 = 0$ and $r_1 \neq 0$. In this case, (48) results in $a_3 = a_4 = 0_M$ while (49) results in $a_1 = a_2 = 0_M$ following from property 1.

Case 4: $r_1 = 0$, $r_2 \neq 0$ and $r_3 \neq 0$. In this case, (48) can be written as $a_1 + \Gamma a_3 = -\frac{r_2}{r_3} a_2$ implying that $a_3 = 0_M$ following from property 2 since $-\frac{r_2}{r_3} \neq 0$. In the same way, (49) can be written as $a_3 + \Gamma a_4 = -\frac{r_3}{r_2} a_2$ resulting in $a_4 = 0_M$ from property 2. Now replacing $a_3 = a_4 = 0_M$ in (49) results in $a_2 = 0_M$. Finally, replacing $a_2 = a_3 = a_4 = 0_M$ in (50) results in $a_1 = 0_M$. Case 5: $r_2 = 0$, $r_1 \neq 0$ and $r_3 \neq 0$. In this case, (50) implies that $a_3 = a_4 = 0_M$ following from property 1. Replacing $r_2 = 0$, $a_3 = 0_M$ and $a_4 = 0_M$ in (48) results in $a_1 = 0_M$. Now (49) can be written as $\Gamma a_2 = -\frac{r_3}{r_1} a_2$ which admits the unique solution $a_2 = 0_M$ over the set $\mathcal{A}$ since no nonzero element of $\Gamma\mathcal{A}$ can be proportional to a nonzero element of $\mathcal{A}$ as highlighted in the proof of property 1. Case 6: $r_3 = 0$, $r_1 \neq 0$ and $r_2 \neq 0$. In this case, (50) results in $a_1 = a_2 = 0_M$ following from property 1. Replacing $r_3 = 0$, $a_1 = 0_M$ and $a_2 = 0_M$ in (49) results in $a_3 + \Gamma a_4 = 0_M$ implying that $a_3 = a_4 = 0_M$ from property 1.

Case 7: $r_1 \neq 0$, $r_2 \neq 0$ and $r_3 \neq 0$. Eliminating the term $(a_1 + \Gamma a_2)$ from (49)-(50) results in:

$$a_2 = \frac{r_1 r_3 - r_2^2}{r_2 r_3}(a_3 + \Gamma a_4) \tag{51}$$

Two possibilities arise in this case. Assume that $r_2^2 = r_1 r_3$. (51) results in $a_2 = 0_M$. Replacing $a_2 = 0_M$ in (50) implies that $a_3 + \Gamma a_4 = -\frac{r_2}{r_3} a_1$ resulting in $a_4 = 0_M$ from property 2 since $-\frac{r_2}{r_3} \neq 0$. On the other hand, if $r_2^2 \neq r_1 r_3$, (51) implies that $a_4 = 0_M$ following from property 2 since $\frac{r_1 r_3 - r_2^2}{r_2 r_3} \neq 0$ in this case. Replacing $a_4 = 0_M$ in (50) implies that $a_1 + \Gamma a_2 = -\frac{r_3}{r_2} a_3$ resulting in $a_2 = 0_M$ from property 2 since $-\frac{r_3}{r_2} \neq 0$. Consequently, both of the above possibilities result in $a_2 = a_4 = 0_M$. Replacing in (48) results in $a_1 + \Gamma a_3 = -\frac{r_1}{r_3} a_3$ implying that $a_3 = 0_M$ from property 2. Finally, replacing $a_2 = a_3 = a_4 = 0_M$ in (49) results in $a_1 = 0_M$.

As a conclusion, in all of the above seven cases, $\mathrm{rank}(C) < 3$ if and only if $a_1 = a_2 = a_3 = a_4 = 0_M$ implying that associating the codewords in (40) with the matrices in (37) or (38) results in a fully-diverse distributed scheme completing the proof of proposition 2.

REFERENCES

[1] J. Laneman and G. Wornell, "Distributed space time coded protocols for exploiting cooperative divesrity in wireless networks," *IEEE Trans. Inf. Theory*, vol. 49, no. 10, pp. 2415–2425, October 2003.

[2] B. Rankov and A. Wittneben, "Spectral efficient protocols for half-duplex fading relay channels," *IEEE J. Sel. Areas Commun.*, vol. 25, no. 2, pp. 379 – 389, February, 2007.

[3] K. Azarian, H. El Gamal, and P. Schinter, "On the achievable diversity-multiplexing tradeoffs in half-duplex cooperative channels," *IEEE Trans. Inf. Theory*, vol. 51, no. 12, pp. 4152–4172, December 2005.

[4] S. Yang and J.-C. Belfiore, "Optimal space-time codes for the MIMO amplify-and-forward cooperative channel," *IEEE Trans. Inf. Theory*, vol. 53, no. 2, pp. 647–663, February 2007.

[5] H. Ju, E. Oh, and D. Hong, "Catching resource-devouring worms in next-generation wireless relay systems," *IEEE Commun. Mag.*, vol. 47, no. 9, pp. 58 – 65, September, 2009.

[6] V. R. Cadambe and S. A. Jafar, "Degrees of freedom of wireless networks with relays, feedback, cooperation, and full duplex operation," *IEEE Trans. Inf. Theory*, vol. 55, no. 5, pp. 2334 – 2344, May, 2009.

[7] Y. Y. Kang and J. H. Cho, "Capacity of MIMO wireless channel with full-duplex amplify-and-forward relay," in *Proceedings IEEE Int. Conf. on Personal, Indoor and Mobile Radio Commun.*, September 2009, pp. 117–121.

[8] T. Kwon, S. Lim, S. Choi, and D. Hong, "Optimal duplex mode for DF relay in terms of the outage probability," *IEEE Trans. Veh. Technol.*, vol. 59, no. 7, pp. 3628 – 3634, September, 2010.

[9] T. M. Kim and A. Paulraj, "Outage probability of amplify-and-forward cooperation with full duplex relay," in *Proceedings IEEE Wireless Communications and Networking Conference*, 2012, pp. 75–79.

[10] T. Riihonen, S. Werner, and R. Wichman, "Hybrid full-duplex/half-duplex relaying with transmit power adaptation," *IEEE Trans. Wireless Commun.*, vol. 10, no. 9, pp. 3074 – 3085, September, 2011.

[11] I. Krikidis, H. A. Suraweera, S. Yang, and K. Berberidis, "Full-duplex relaying over block fading channel: a diversity perspective," *IEEE Trans. Wireless Commun.*, vol. 11, no. 12, pp. 4524 – 4535, December, 2012.

[12] I. Krikidis and H. A. Suraweera, "Full-duplex cooperative diversity with Alamouti space-time codes," *IEEE Wireless Commun. Lett., accepted for publication*.

[13] Y. Liu, X.-G. Xia, and H. Zhang, "Distributed space-time coding for full-duplex asynchronous cooperative communications," *IEEE Trans. Wireless Commun.*, vol. 11, no. 7, pp. 2680 – 2688, July, 2012.

[14] K. Maichalernnukul, T. Kaiser, and F. Zheng, "On the performance of coherent and noncoherent UWB detection systems using a relay with multiple antennas," *IEEE Trans. Wireless Commun.*, vol. 8, no. 7, pp. 3407 – 3414, July 2009.

[15] Z. Zeinalpour-Yazdi, M. Nasiri-Kenari, and B. Aazhang, "Bit error probability analysis of UWB communications with a relay node," *IEEE Trans. Wireless Commun.*, vol. 9, no. 2, pp. 802 – 813, February 2010.

[16] Z. Zeinalpour-Yazdi, M. Nasiri-Kenari, B. Aazhang, J. Wehinger, and C. Mecklenbrauker, "Bounds on the delay-constrained capacity of UWB communication with a relay node," *IEEE Trans. Wireless Commun.*, vol. 8, no. 5, pp. 2265 – 2273, May 2009.

[17] M. Mondelli, Z. Qi, V. Lottici, and M. Xiaoli, "Joint power allocation and path selection for multi-hop noncoherent decode and forward UWB communications," *IEEE Trans. Wireless Commun.*, vol. 13, no. 3, pp. 1397 – 1409, March 2014.

[18] K. Maichalernnukul, F. Zheng, and T. Kaiser, "Design and performance of dual-hop MIMO UWB transmissions," *IEEE Trans. Veh. Technol.*, vol. 59, no. 6, pp. 2906 – 2920, July 2010.

[19] M. Hamdi, J. Mietzner, and R. Schober, "Multiple-differential encoding for multi-hop amplify-and-forward IR-UWB systems," *IEEE Trans. Wireless Commun.*, vol. 10, no. 8, pp. 2577 – 2591, August 2011.

[20] C. Abou-Rjeily, N. Daniele, and J. C. Belfiore, "On the amplify-and-forward cooperative diversity with time-hopping ultra-wideband communications," *IEEE Trans. Commun.*, vol. 56, no. 4, pp. 630 – 641, April 2008.

[21] C. Abou-Rjeily and W. Fawaz, "Distributed information-lossless space-time codes for amplify-and-forward TH-UWB systems," *IEEE Commun. Lett.*, vol. 12, no. 4, pp. 298 – 300, April 2008.

[22] J. Foerster, "Channel modeling sub-committee Report Final," Technical report IEEE 802.15-02/490, IEEE 802.15.3a WPANs, 2002.

[23] I. Krikidis, H. A. Suraweera, P. J. Smith, and C. Yuen, "Full-duplex relay selection for amplify-and-forward cooperative networks," *IEEE Trans. Wireless Commun.*, vol. 11, no. 12, pp. 4381 – 4393, December, 2012.

[24] M. O. Damen and A. R. Hammons, Jr., "Delay-tolerant distributed-TAST codes for cooperative diversity," *IEEE Trans. Inf. Theory*, vol. 53, no. 10, pp. 3755–3773, October 2007.

[25] C. Abou-Rjeily, "A maximum-likelihood decoder for joint pulse position and amplitude modulations," in *Proceedings IEEE Int. Conf. on Personal, Indoor and Mobile Radio Commun.*, September 2007.

[26] V. Tarokh, N. Seshadri, and A. Calderbank, "Space-time codes for high data rate wireless communication : Performance criterion and code construction," *IEEE Trans. Inf. Theory*, vol. 44, pp. 744–765, 1998.

[27] C. Abou Rjeily, N. Daniele, and J. C. Belfiore, "Diversity-multiplexing tradeoff of single-antenna and multi-antenna indoor ultra-wideband channels," in *Proceedings IEEE Conference on UWB*, September 2006, pp. 441 – 446.

[28] C. Abou-Rjeily, "Performance analysis of UWB systems over the IEEE 802.15.3a channel model," *IEEE Trans. Commun.*, vol. 59, no. 9, pp. 2377–2382, September 2011.

[29] J. G. Proakis, *Digital Communication*. New York: McGrawHill, 4th edition 2000.